Environmental Health Engineering and Management Journal 2022, 9(4), 365-374
http://ehemj.com
doi 10.34172/EHEM.2022.39

Environmental Health Engineering and Management Journal

Original Article

Environmental Health Engineering and Management

Open Access Publish Free

Investigation of toxicity of TiO_2 nanoparticles on glioblastoma and neuroblastoma as the most widely used nanoparticles in photocatalytic processes

Fahimeh Kazemi[1], Marzie Esmaeeli[2], Peyman Mohammadzadehjahani[1], Mahnaz Amiri[2], Parisa Vosough[2], Meysam Ahmadi-Zeidabadi[2*]

[1]School of Medicine, Bam University of Medical Sciences, Bam, Iran
[2]Neuroscience Research Center, Institute of Neuropharmacology, Kerman University of Medical Sciences, Kerman, Iran

Abstract

Background: Titanium dioxide (TiO_2) nanoparticles (NPs) are among the most important and usable photocatalysts. Recently, the biological properties of these NPs, particularly, its anticancer activity, have been considered. Glioblastoma and neuroblastoma are two fatal brain tumors with a high mortality rate in humans, the hope for treatment of which is weak by the common methods.

Methods: In this study, the cytotoxicity effects of TiO_2 alone and in combination with ultraviolet A (UVA) irradiation on two different cell lines, neuroblastoma (SH-SY5Y) and glioblastoma U87, were investigated. After administration of 10, 50, 100, and 500 µg/mL TiO_2, 0.043 and 1.4 mW/cm^2 UVA irradiation, cell viability was investigated after 4, 24, and 48 hours by 3-(4,5-dimethylthiazol-2-yl)-2,5-diphenyltetrazolium bromide (MTT) assay.

Results: MTT assay and light microscope demonstrated that the effect of TiO_2 NPs varied based on the dose of the substance, the impact time, the cell type, and the amount of radiation. In this study, for NPs alone, both toxicity and non-toxicity of the substance were observed. For NPs in the presence of UV, based on the comparison with its status alone and the difference in the viability assay of the two groups, both the photocatalytic and the coating effect of the NPs were observed.

Conclusion: According to the results, different concentrations of TiO_2 can be used for different purposes. Low concentrations of TiO_2 can be used to increase the efficiency of photodynamic therapy and high concentrations of TiO_2 can be used to protect the normal cell. This strategy improves the photodynamic therapy and reduces the harmful effects.

Keywords: Titanium, Nanoparticles, UV radiation, Neuroblastoma, Glioblastoma

Citation: Kazemi F, Esmaeeli M, Mohammadzadehjahani P, Amiri M, Vosough P, Ahmadi-Zeidabadi M. Investigation of toxicity of TiO_2 nanoparticles on glioblastoma and neuroblastoma as the most widely used nanoparticles in photocatalytic processes Environmental Health Engineering and Management Journal 2022; 9(4): 365-374. doi: 10.34172/EHEM.2022.39.

Article History:
Received: 3 January 2022
Accepted: 30 April 2022
e Published: 18 December 2022

***Correspondence to:**
Meysam Ahmadi-Zeidabadi,
Email: meysamcell@yahoo.com, m.ahmadi@kmu.ac.ir

Introduction

Nanostructures have gained different applications in biomedical investigations (1). Currently, cancer threatens overall health of the community (1). In 2018, there were 18.1 million cancer cases and about 9.6 million people died from cancer. With the continuous emergence of smart therapy and immunotherapy, inventive oncology has made dramatic progress. However, the relative living rate of cancer patients has had a lot of progress and the inevitability human death speed of cancer has reduced. Most treatments for cancer, are often accompanied by violent and sometimes irremovable side effects, however, definitive treatment for this disease is difficult. For this reason, there is an urgent need to discover a quick and safe cure for this mysterious disease (2-4).

Titanium dioxide (TiO_2) nanoparticles (NPs) are one of the main photocatalysts that have various fields of application, including self-cleaning surfaces, wastewater treatment, pigments, etc. TiO_2 is excited in the presence of UV and produces free electrons, which lead to the production of free radicals (O_2^-, OH, H_2O_2). TiO_2 can also be used as a coating against UV, which is also used in sunscreens (5-7). Due to the increased permeability and maintenance effect, nanomaterials tend to passively collect in tumor cells, and often, act as nanocarriers of chemotherapeutic agents (8). Semiconductor TiO_2 is a usual photocatalyst material, which is generally used to ravage organic materials (9), demobilize microorganisms (10) and bacteria (11). Some research reported TiO_2 NPs of several sizes and patterns exhibited cytotoxicity

against tumors (12-14). The catalytic activity of the photocatalysts achieved by photon energy can oxidize or reduce materials. In many cases, photocatalysts have been used as antibacterial and antiviral agents (15,16).

In recent years, many studies have been conducted on the capabilities and value of photocatalysts in cancer therapy. Zhang et al (17) designed a supramolecular photocatalyst of tetracarboxyphenyl porphyrin (SA-TCPP) and demonstrated that it can be excited by the wavelength of 420-750 nm. Porphyrin-based agents are largely used in PDT based on their great biocompatibility and release of singlet oxygen, some of which have achieved medical applications. Yi et al (18) reported that photocatalytic agents can produce ROS for tumor DNA destruction when they are exposed to the targeted wavelength light, achieving high performance at low radiation levels with moderate damages to normal tissues.

In general, NPs interaction with the cells has different effects depending on the type, size, phase, amount of agglutination, and cell type. Based on these parameters, cell infiltration can also be different (19). TiO_2 is no exception for this rule (20). Research shows that the photocatalytic effect of titanium can also depend on the amount of substance and agglutination, and at high doses (in solution), its photocatalytic properties can be suppressed (21). Recently, the biological properties of this nanoparticle, in particular, its anticancer activity, have been considered. TiO_2 NPs have been observed in different types of cancer cells such as mesenchymal stem cells, lymphoblastoid breast (22,23), lung (24), epidermal (25,26), and colon (27) cancer cells.

Glioblastoma and neuroblastoma are two fatal brain tumors with high mortality rate in humans. The hope for treatment of these types of cancer by the common methods, such as surgery, chemotherapy, and radiation therapy, is weak (28).

Photodynamic therapy (PDT) has been reported as a useful treatment for brain cancer. In PDT, if transmission of the photosensitizer to the target tumor is managed and the radiation is completely localized, many harmful effects on the cells are reduced or eliminated (29,30). Usually, the PDT method entails three main constituents including light, oxygen, and light-responsive materials (photosensitizers). Hybrid semiconductor photocatalysts attract energy from light, and then, transfer it to molecular oxygen to produce cytotoxic reactive oxygen species (ROS) (31). The advantages of nanophotocatalysts are the results of the synergistic combination of inorganic agents with unique physical characteristics and the targeting performance of cancer cells (32). Moreover, nanophotocatalysts can cross through biological barriers, including the blood-brain barrier. In recent years, some studies has been conducted on cancer treatment using the photocatalytic property of TiO_2 and electron excitation in the presence of UV, including the simultaneous study of TiO_2 and UV on the brain cancer cells (21,33).

The present research aimed to investigate the effect of TiO_2 NPs (rutile phase-30 nm) alone, UV radiation (0.043 and 1.4 mW/cm^2), and the simultaneous effect of NPs and UV radiation on glioblastoma cells (U87) and neuroblastoma cells (SH-SY5Y).

Materials and Methods

Tio$_2$ preparation and administration

TiO_2 (CAS# 13463-67-7 Lot no: Tl-C4L29.1/101400125) nanostructures with a rutile phase and 30 nm size were purchased from Tecnac company (Spain). The NPs were dissolved in PBS, sonicated by a sonic instrument with a power of (Sonopuls Ultrasonic homogenizer HD 2070, Bandelin electronic, Berlin, Germany) at 45% of amplitude for five cycles, each set for 12 seconds followed by 6 s pause, on ice. For better uniformity and non-precipitation formation, the solution was vortexed well every time before use. It was used at various concentrations of 10, 50, 100, and 500 μg/mL. Each group including 4 wells were considered as: 1) control-no treatment, 2) treatment with UV irradiation alone (UV), 3) treatment with 10, 50, 100, and 500 μg/mL TiO_2 concentration (T10, T50, T100, T500), 4) combination of the UV and TiO_2 treatments at 10, 50, 100, and 500 μg/mL concentration (T10 + UV, T50 + UV, T100 + UV, T500 + UV). The treatment with TiO_2 and exposure were performed 24 hours after seeding.

Cell culture

Glioblastoma cells line U87 and neuroblastoma cells line SH-SY5Y (Pasteur Institute, Tehran, Iran) were cultured in 50 cm^2 flasks (Iwaki, Tokyo, Japan) at a cell density of $5*10^4$ cells/mL in Dulbecco's modified Eagle's medium (DMEM; Invitrogen Inc. Gibco BRL, Gaithersburg, MD, USA). The cultures were supplemented with 10% (v/v) inactivated fetal bovine serum (FBS, Product Code: 12306C-500ML, Sigma-Aldrich Co., St. Louis, MO, USA) and 1% (v/v) of penicillin/streptomycin solution (Product Code: P4333-100ML, Sigma-Aldrich Co.) and incubated in an atmosphere of 5% CO_2 at 37 ± 0.2°C. The medium was replaced every 2 days. Cell cultures with 80% confluence were routinely trypsinized (Product Code of Trypsin: T4549-100ML, Sigma-Aldrich Co.) and seeded 10^4 cells in each well of the 96-well plates.

Cytotoxicity studies

To determine the effect of TiO_2 (rutile phase-30 nm) and UV irradiation (0.043 mW/cm^2) on the viability rate, 10^4 cells of U87 and SH-SY5Y cell line per each well of 96-well plates were seeded. The first group of cells was irradiated with UV-A exposure (UV group), and the second one was treated with different concentrations of TiO_2 (10, 50, 100, and 500 μg/mL) in dark condition. To examine the effects of NPs and UV concomitantly, the administration of both groups and the lethal effects were analyzed after 4,

24, and 48 hours. The cell death rate was measured using the MTT assay. Cellular morphology was also performed using an optical microscope.

UV Exposure system

The UV-A lamp (Actinic BL TL(-K)/TL-D(-K), Philips, Holland) was used as the exposure source. The irradiation wavelength range was 300-400 nm at the peak of 365 nm. The exposure system was designed and made in a way that it was able to locate within CO_2 incubator and provided the desired uniform distribution intensity of irradiation at the plate position. The intensity of UV irradiation at the plate position were 1.4, 0.062, and 0.043 mW/cm^2, according to the UV lamp position with a 30-min duration for both UV and TiO_2 + UV groups. Figure 1 indicates the UV exposure system.

The UV radiation system was made of two fixed plates and one moving plate and it had three steps, at intervals of 10-15 and 18 cm from the surface of cell plate.

The intensity of radiation on the vials surface was calculated by the following formula:

$$\frac{I_2}{I_1} = \frac{r_1^2}{r_2^2}$$

The radiant power of lamp according to its catalog was 1.4 W and the radiant powers at distances 10-15 and 18 cm were calculated to be 1.4-0.062, and 0.043 mW/cm^2, respectively.

Light microscopy

To investigate morphological cellular changes, an inverted phase-contrast microscope (Carl Zeiss AG, Oberkochen, Germany) was used.

Viability assay

The effect of TiO_2 treatment and UV exposure on the viability of U87 and SH-SY5Y cells was assessed by the 3-(4,5-dimethylthiazol-2-yl)-2,5-diphenyltetrazolium bromide (MTT) dye reduction assay, in which dye crystals are produced by mitochondria of living cells (34). The MTT assay was done according to the modified method described by Sladowski et al (35). The cells in each well of 96-well plates were incubated for 2 hours with 1 mg/mL of MTT in DMEM at 37°C with 5% CO_2. After washing the cells two times with 0.2-M PBS at pH 7.4, the reduced MTT formazan crystals were solubilized in 200 µL of DMSO. Then, the optical density was read by an enzyme-linked immunosorbent assay (ELIZA) reader at 570 nm.

Living cells analysis by 3-(4,5-dimethylthiazol-2-yl)-2,5-diphenyltetrazolium bromide

In this step similar to the previous one, the 3-(4,5-dimethylthiazol-2-yl)-2,5-diphenyltetrazolium bromide reagent was used. But with a different approach, the amount of living cells was evaluated qualitatively and schematically. Formazan crystals formed in viable cells. Using this technique, living cells under TiO_2 sediment could be observed.

Statistical analysis

The collected data were analyzed using SPSS version 16 (IBM, Armonk, NY, USA). Data were presented as standard error of the mean (FE-SEM). The difference between treated vs. control groups was investigated by the student's *t* test at the 95% confidence interval. One-way analysis of variance (ANOVA) method was used to compare different groups. *P* values less than 0.05 were considered significant.

Treatment of cell with TiO_2, UV, and TiO_2 + UV

To determine the effect of TiO_2 (rutile phase-30 nm) and UV irradiation (0.043 mW/cm^2) on the viability rate, 10^4 cells of U87 and SH-SY5Y cell line per each well of 96-well plates were seeded. The first group of cells was irradiated with UV-A exposure (UV group), and the second one was

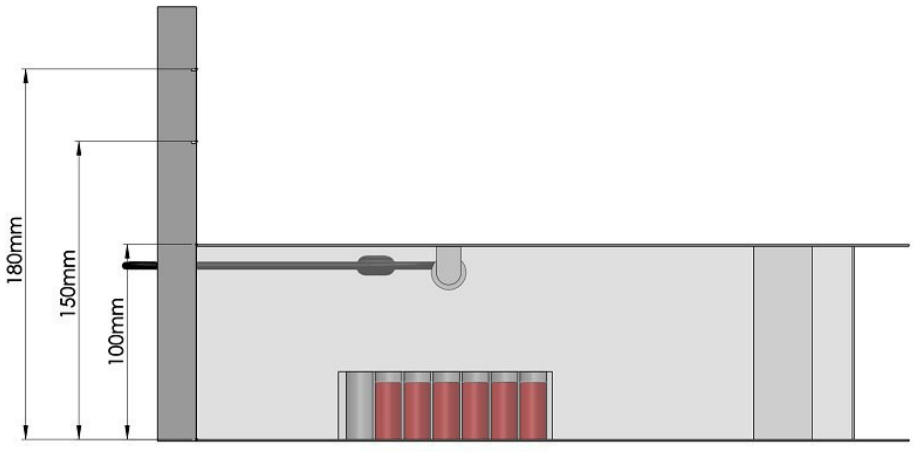

Figure 1. UV exposure system

treated with different concentrations of TiO_2 (10, 50, 100, and 500 µg/mL) in dark condition. To examine the effects of NPs and UV concomitantly, the administration of both groups and the lethal effects were analyzed, after 4, 24, and 48 hours. The cell death rate was measured using the MTT assay. Cellular morphology was also performed using an optical microscope.

TiO_2 characterization

The diagram of Amp Vs Rh (hydrodynamic radius) in nanometer range shows the average radius of suspended particles as 215 nm, indicating the presence of nano-sized TiO_2 particles (Figure 2A). The real size of NPs is not clear; therefore, particle size was calculated by Nanosizer cordouan (France) and the results revealed that the mean particle size with hydrodynamic radius is 215 nm in diameter. The reported results indicate that TiO_2 NPs provide homogenous dispersity and narrow size distribution. The FTIR spectrum of bare TiO_2 NPs (Figure 2B) showed a wide, broad band at 3200-3500 cm^{-1} due to the stretching vibration of water molecules adsorbed on the surface of hydrophilic TiO_2 NPs. The small peak at 1650 cm^{-1} was attributed to AOH bending vibrations. Many peaks below 700 cm^{-1} were present because of the numerous TiAOATi bonds in bare TiO_2 NPs. The particles are spherical and the size estimated from FE-SEM was found to be in the range of 30-50 nm (Figure 2C).

Results

Cytotoxicity of UV exposure at a low-dose (0.043 mw/cm_2) intensity on U87 and SH-SY5Y

Viability assay was investigated 4, 24, and 48 h after UV irradiation, by the MTT test and cellular morphology. Data showed that UV radiation for (30 minutes duration and 0.043 mW/cm^2 intensity) decreased viability about 17% for U87 but in SH-SY5Y cell line, it remained constant without any changes in the viability assay after 4 hours. After 24 hours, U87 viability was equal to the control group in despite of SH-SY5Y cells that the viability decreased to 90%. After 48 h, both of the cells return to the normal situation, as control (Figure 3A and 3B).

Cytotoxicity of TiO_2 on U87 and SH-SY5Y

After TiO_2 treatment at different doses (10, 50, 100, and 500 µg/mL), viability assay was performed by the MTT test after 4, 24, and 48 hours incubation time. Data obtained after 4 hours demonstrated that viability decreased about 10%, 7%, and 4%, respectively, for T10, T100, and T500 groups of U87 but in SH-SY5Y cells, it remained constant without any changes for all TiO_2 concentration. After 24 hours, U87 viability decreased 10%, 21%, and 11% compared to control. In SH-SY5Y cell line, viability was reported 92%, 94%, and 105% compared to control. After 48 hours, viability decreased about 10%, 18%, and 0%. Surprisingly, in SH-SY5Y cells, no changes were detected (Figure 3C and 3D).

Cytotoxicity of concomitant treatment of TiO_2 and UV on U87 and SH-SY5Y

In concomitant administration of TiO_2 and UV irradiation, data showed that after 4 hours, U87 cells viability reached 79%, 77%, and 90%, for T10 + UV, T100 + UV, and T500 + UV groups, respectively. At the same time, SH-SY5Y cells viability reduced only about 10% in T10 + UV compared to control. After 24 hours, the viability of U87 cells reduced 89%, 84% for T10 + UV and T100 + UV groups, respectively, but without any changes in T500 + UV group. In SH-SY5Y, viability decreased 10% in T10 + UV and T100 + UV groups and T500 + UV did not change compared to control group. Surprisingly, both of cells recover to normal status vs control (Figures 4A and 4B).

Cytotoxicity of concomitant treatment of TiO_2 and UV) at a high-dose intensity of 1.4 mW/cm^2(on U87

According to previous steps, U87 cell was found to be more sensitive to UV and TiO_2 administration. So, the high-dose UV irradiation was used to investigate the interaction between UV and titanium accurately.

Data showed that low concentrations of titanium become more toxic in the presence of UV about 20%, but high concentrations of titanium not only reduce its toxicity but also protect the cell against UV toxicity about 40% (Figure 4C).

Morphological analysis

The morphology of U87 and SH-SY5Y cells were monitored during the experiments using a light microscope. 3-(4,5-dimethylthiazol-2-yl)-2,5-diphenyltetrazolium bromide is a yellow dye, which is reduced by cellular mitochondria enzymes to the purple product formazan. Because the transformation is only possible in viable cells, the amount of purple formazan is proportional to the number of cells. Also, it was used to prove the activity of these cells. After UV irradiation, two kinds of cells respond differently, U87 was very sensitive to the UV exposure, the number and viability of cell decrease dramatically. While in the SH-SY5Y cells, there was no significant difference in color intensity and cell number (Figure 5).

The amount of titanium penetration is different in two kinds of cells. This difference is related to cell type, concentration of titanium, and exposure intensity. Titanium passed through the cell membrane of the U87 cells but it was not able to enter the SH-Sy5Y cells. In addition, titanium penetrates at lower concentrations. As concentration increased, its penetration and toxicity decreased (Figure 6).

Surprisingly, at high concentration of 500 µg/mL, not only the toxicity of titanium was greatly reduced, but also, maybe titanium acted as a protective shield and neutralized

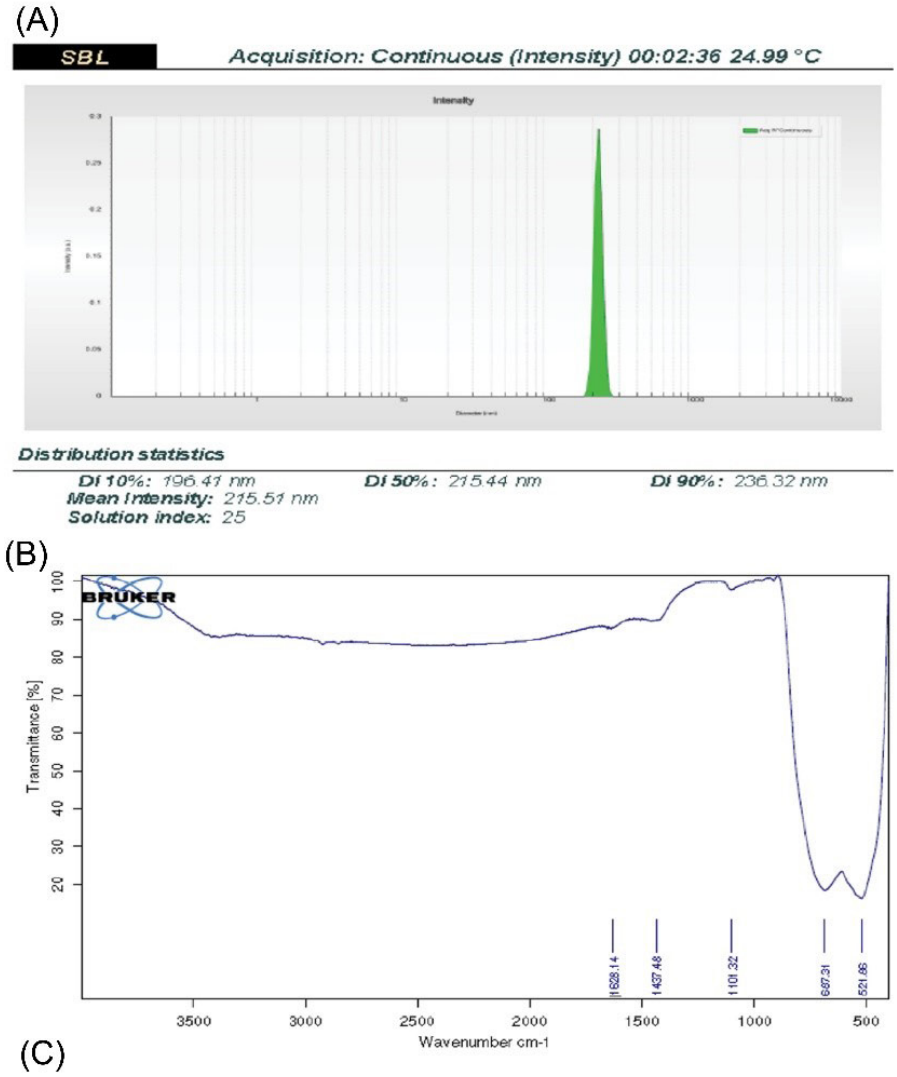

Figure 2. DLS size (A), FTIR pattern (B), and FE-SEM image (C) of nanostructured TiO_2

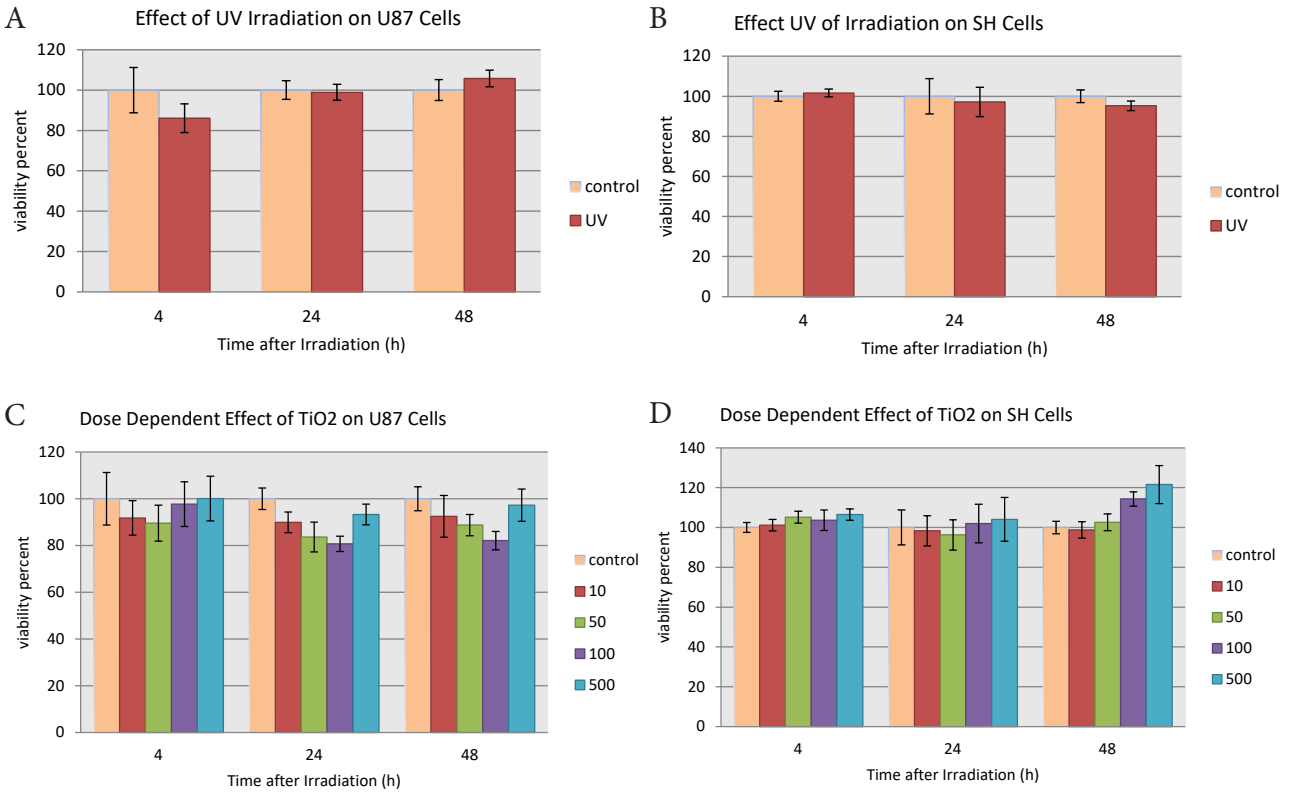

Figure 3. Effect of UVA (30 min, 0.043 mW/cm^2) on U87 and SH-SY5Y cells viability and cytotoxicity of TiO_2 NPs in human glioblastoma (U87) (C) and neuroblastoma (SH-SY5Y) (D) cells by the MTT assay. The viability of the control cells was considered to be 100%. The data are expressed as mean ± SEM from three independent experiments. Asterisk indicates a significant difference compared to control group ($P \leq 0.05$).

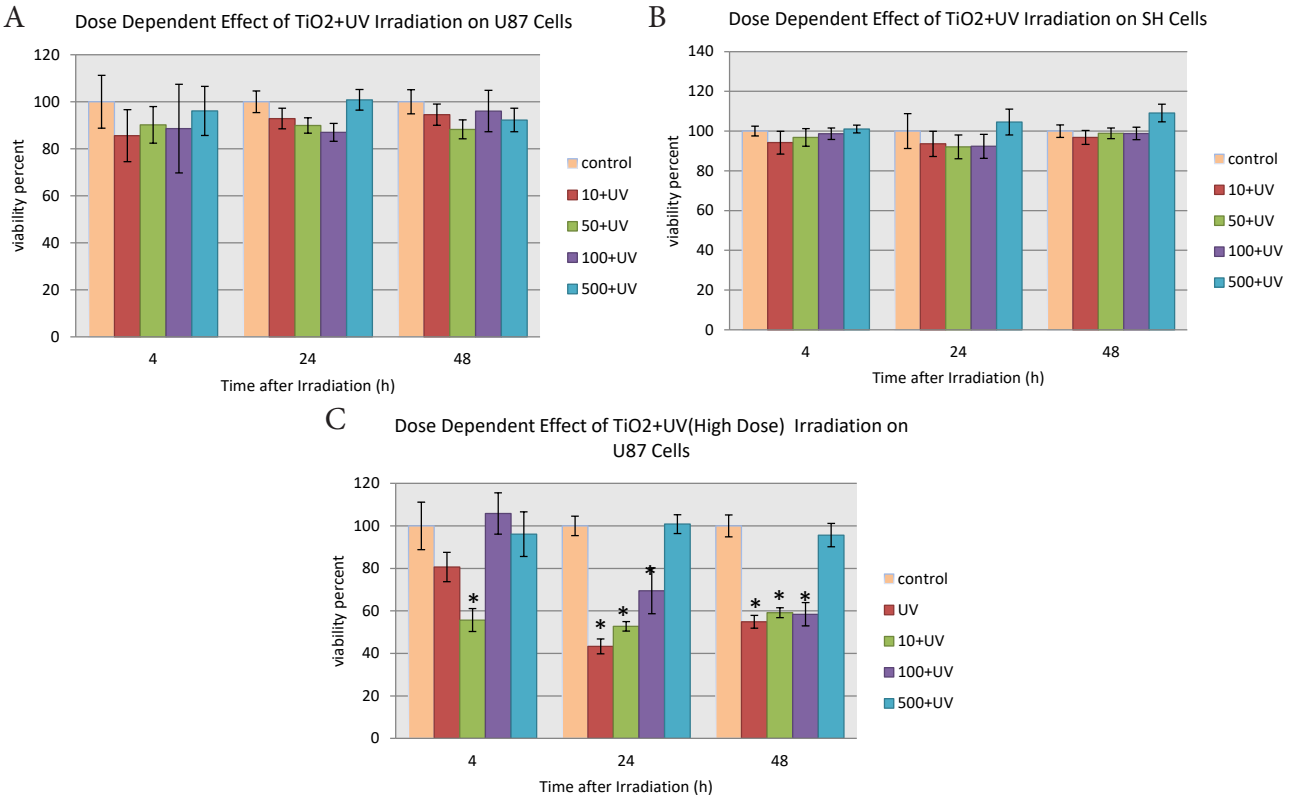

Figure 4. Viability assay after coadministration of Nano-TiO_2 (10, 50, 100, and 500 µg/mL) and UVA (0.043 mW/cm^2, 30 min) in human glioblastoma (U87) (A) and neuroblastoma (SH-SY5Y) (B) and coadministration of Nano-TiO_2 (10, 100, and 500 µg/mL) and UVA (1.4 mW/cm^2, 30 min) in human glioblastoma (U87) (C) cells by the MTT assay. Asterisk indicates a significant difference compared to control .

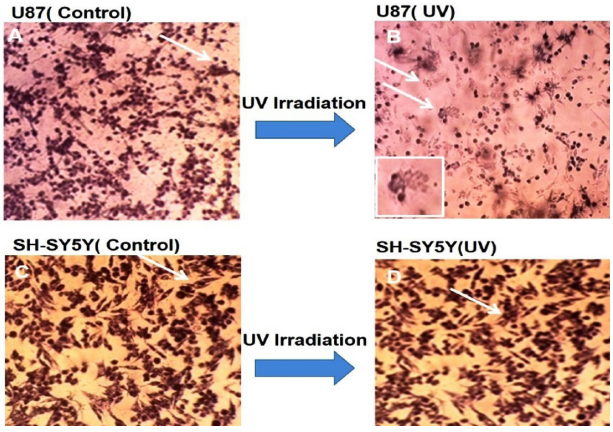

Figure 5. LM micrographs of U87 and SH-SY5Y cells under the UV exposure condition. The representative morphological changes after 4 h exposure to UVA (0.043 mW/cm^2, 30 min). A) control (U87), the arrows show purple cells, which represent living and active cells; B) U87 treated by UV exposure, the arrows show small and colorless cells, which indicates inactive and dead cells; C) SH-SY5Y (Control) cells; D) SH-SY5Y (UV). In both figure (C and D), the arrows represent live and active cells, which are seen in purple color. Magnification: 40X.

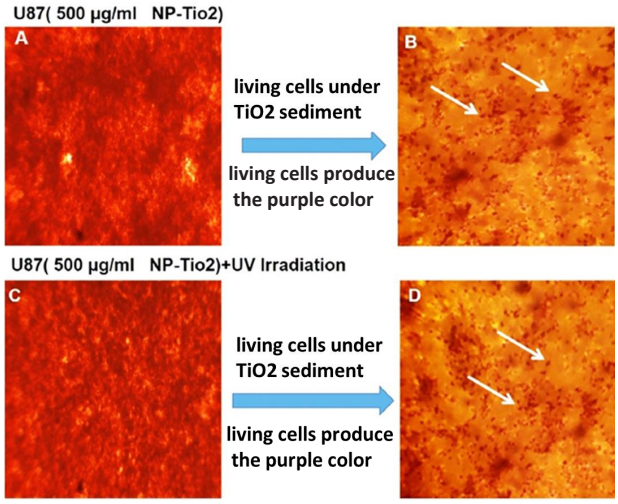

Figure 7. The LM micrographs of U87 cells under UV exposure and UV + TiO_2 conditions. (A and C) Cells after 48 h administration of NP-Tio_2 (500 µg/mL). In Figure A, TiO_2 covers cells and cells are not visible but in Figure B and D, the color of the cells was changed to purple after the addition of 3-(4,5-dimethylthiazol-2-yl)-2,5-diphenyltetrazolium bromide. And the cells were visible below the sediment. Magnification: 40X.

the lethal effects of UV radiation. 3-(4,5-dimethylthiazol-2-yl)-2,5-diphenyltetrazolium bromide was used to observe live cells under titanium deposition (Figure 7).

Discussion

The aim of this study was to find a new approach for treatment of cancer according to the TiO_2 photocatalytic properties. The present research for TiO_2 with a rutile phase and 30 nm size was performed on two cell lines U87 and SH-SY in two states, NPs alone and in the presence of UV. The results demonstrated that the effect of TiO_2 NPs in both cases, alone and in the presence of UV, depends on the cell type, amount of material, radiation intensity, and impact time, and in both cases, U87 cell was more sensitive than SH-SY. The findings of the present study demonstrate that likely photocatalytic property of TiO_2 is closely related to TiO_2 concentration. TiO_2 at low concentrations is toxic and its toxicity increased in combination with UV. Adversely, TiO_2 at high concentrations is less toxic, in addition, it can be said that TiO_2 at high concentrations protect the cells against UV.

Based on the results, the effect of titanium NPs, both alone and in the presence of UV, depends on the cell type, the amount of radiation, and the impact time. As the data show, the results vary based on the differences in these

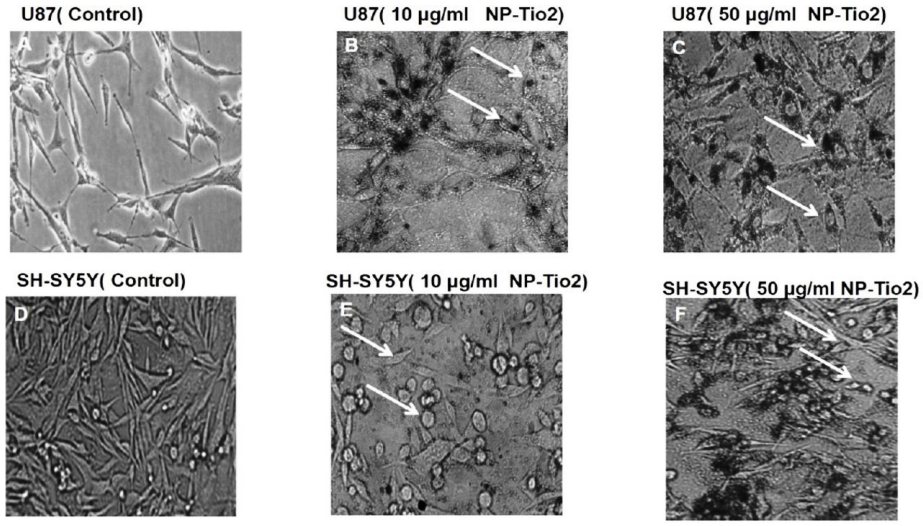

Figure 6. LM micrographs of U87 and SH-SY5Y cells under different concentrations of Tio_2. The representative morphological changes after 4 h exposure to 10, 50 TiO_2 NPs. A) control U87; B and C) U87 cells that exposed to 10 and 50 TiO_2, respectively, the amount of titanium penetration is different in two kinds of cells. This difference is related to cell type, and concentration of titanium. Titanium passed through the cell membrane of the U87 and localized in different compartment of cell according to concentration shown by arrow. D) control SH-SY5Y, E and F) SH-SY5Y cells that exposed to 10 and 50 TiO_2, respectively. But, titanium was not able to enter the SH-Sy5Y cells. The arrows show the clear cells without any TiO_2 sedimentation. Magnification: 200X.

parameters.

For U87 cells, in general at low doses (especially at dose of 10 μg/mL) in both cases, the NPs alone and in the presence of UV, a greater effect was observed. At high doses (500 μg/mL), the effect was not so noticeable.

This difference can be attributed to the amount of substance and agglutination, which at low doses, due to the lack of agglutination, the substance can penetrate more into the cell, and at high doses, the substance due to the amount of agglutination cannot penetrate into the cell.

At a low dose (10 μg/mL) in the presence of UV, the substance is activated and the photocatalytic effect was observed, and at dose of 500 μg/mL, the cessation of the photocatalytic and the coating effect of the substance was observed. For SH cells, not much effect was reported in almost all cases.

Some data have reported the effects of TiO_2 NPs and UV exposure on cancer cells, including brain cancer cells. Cai et al reported that TiO_2 NPs effectively killed HeLa cells with UV irradiation (36).

Wang et al reported that combined TiO_2 + UVA treatment can significantly reduce glioma growth, whereas 200 μg/mL TiO_2 irradiated by 5 J/cm^2 UVA about 60% inhibited U87 proliferation in vitro, which is consistent with the results of the present study (33).

Yamaguchi et al reported that the TiO_2/PEG nanoparticle was not toxic for the rat glioma cell line (C6) within the range of 0-500 μg/mL, but the lethal effect increased with higher TiO_2/PEG concentration and longer duration of UV irradiation (13.5 J/cm^2), which is inconsistent with the results of the present study (21).

Stefanou et al also indicated that the aggregation of platelets were efficiently prevented by photoexcited TiO_2 NPs, which led to the discontinuation of hematogenous metastasis (37).

The killing effect of nitrogen-doped TiO_2 NPs in the visible light also has been reported. The electrons in the TiO_2 photocatalyst capacity layer are excited in the presence of UV light with wavelengths less than 400 nm. As a result of this excitation, electron-hole pair is generated, which can induce oxidative stress through the production of anion superoxide (O_2^-), hydrogen peroxide (H_2O_2), and hydroxyl radical (OH) such as ROS (38,39).

Matsunaga et al for the first time reported photocatalytic activity for NPs of TiO_2 (40). When being exposed to radiation UV, the TiO_2 NPs can be photoexcited to produce electron (−CBe) in the conduction band and a positive hole (+VBh) in the valence band. TiO_2 NPs also have been considered as a potential photosensitizing material for PDT. In an aqueous environment, the photo-induced electrons and hole pairs react with oxygen or water to produce ROS such as hydroxyl (HO) and superoxide radical (O_2). These reactive species are actively oxidative and can destroy the structure of various organic molecules, therefore, they have found many applications in the elimination of infectious molecules and organic contamination (27,41).

The ROS produced from the photoexcited TiO_2 NPs can interact with cell membranes and cell organelles, leading to toxic responses and/or death of cell (42). The research generally has been limited to laboratory investigations. The medical application of TiO_2 NPs has been limited by some problems such as insufficient selectivity and low efficiency resulting from the lack of specific accumulation of TiO_2 on cancer cells (14).

According to the results of this study and comparison with other articles, it can be concluded that the effect of TiO_2 NPs on cancer cells depends on the phase, dose, intensity, and duration of radiation. In addition, the concentration of TiO_2 and kind of cells are very important. Based on this research, it can be concluded that the adequate dose of TiO_2 and UV radiation can be used to kill cancer cells, and also, as a coating to protect healthy cells, which is very important for treatment.

Conclusion

In this study, the possibility of reducing the growth of cancerous cells by photoexcited TiO_2 (rutile phase-30 nm) was investigated. The adverse glioma effects of nano-TiO_2 excited with ultraviolet A (UVA) irradiation in vitro were analyzed. Transmission electron microscopy, BET analysis, and DLS nanosizer demonstrated that TiO_2 nanostructures are in a nanometer range under 30 nm. TiO_2 + UVA led to the induction of apoptosis, delayed tumor growth, and increased survival compared with the low concentrations of TiO_2. In conclusion, different concentrations of TiO_2 can be used for different purposes, for example, low concentrations of TiO_2 can be used to increase the efficiency of photodynamic therapy and high concentrations of TiO_2 can be used to protect the normal cell. This strategy improves photodynamic therapy and reduces the harmful effects.

Acknowledgements

The authors would like to thank Bam University of Medical Sciences for its financial support.

Ethics Issues

Not applicable.

Competing interests

The authors declare that there is no conflict of interests.

Authors' contributions

Conceptualization: Meysam Ahmadi-Zeidabadi, Fahimeh Kazemi, Peyman Mohammadzadehjahani.
Data curation: Meysam Ahmadi-Zeidabadi.
Formal Analysis: Marzie Esmaeeli.
Investigation: Fahimeh Kazemi, Parisa Vosough, Meysam Ahmadi-Zeidabadi.

Funding acquisition: Fahimeh Kazemi, Parisa Vosough, Meysam Ahmadi-Zeidabadi.
Methodology: Mahnaz Amiri, Meysam Ahmadi-Zeidabadi.
Project administration: Meysam Ahmadi-Zeidabadi.
Resources: Meysam Ahmadi-Zeidabadi.
Software: Meysam Ahmadi-Zeidabadi.
Supervision: Meysam Ahmadi-Zeidabadi.
Validation: Meysam Ahmadi-Zeidabadi.
Visualization: Meysam Ahmadi-Zeidabadi.
Writing–original draft: Fahimeh Kazemi, Meysam Ahmadi-Zeidabadi, Peyman Mohammadzadehjahani.
Writing – review & editing: Meysam Ahmadi-Zeidabadi.

References

1. Zinatloo-Ajabshir S. Advanced rare earth-based ceramic nanomaterials at a glance. In: Zinatloo-Ajabshir S, ed. Advanced Rare Earth-Based Ceramic Nanomaterials. Elsevier; 2022. p. 1-11. doi: 10.1016/b978-0-323-89957-4.00011-6.
2. Fernández-Ibáñez P, Blanco J, Malato S, de las Nieves FJ. Application of the colloidal stability of TiO2 particles for recovery and reuse in solar photocatalysis. Water Res. 2003;37(13):3180-8. doi: 10.1016/s0043-1354(03)00157-x.
3. Fujishima A, Rao TN, Tryk DA. Titanium dioxide photocatalysis. J Photochem Photobiol C Photochem Rev. 2000;1(1):1-21. doi: 10.1016/s1389-5567(00)00002-2.
4. Shi H, Magaye R, Castranova V, Zhao J. Titanium dioxide nanoparticles: a review of current toxicological data. Part Fibre Toxicol. 2013;10:15. doi: 10.1186/1743-8977-10-15.
5. Smijs TG, Pavel S. Titanium dioxide and zinc oxide nanoparticles in sunscreens: focus on their safety and effectiveness. Nanotechnol Sci Appl. 2011;4:95-112. doi: 10.2147/nsa.s19419.
6. Amirmahani N, Mahmoodi N, Bahramnejad M, Seyedi N. Recent developments of metallic nanoparticles and their catalytic activity in organic reactions. J Chin Chem Soc. 2020;67(8):1326-37. doi: 10.1002/jccs.201900534.
7. Nasrollahzadeh M, Mahmoudi-Gom Yek S, Motahharifar N, Ghafori Gorab M. Recent developments in the plant-mediated green synthesis of Ag-based nanoparticles for environmental and catalytic applications. Chem Rec. 2019;19(12):2436-79. doi: 10.1002/tcr.201800202.
8. Bae KH, Chung HJ, Park TG. Nanomaterials for cancer therapy and imaging. Mol Cells. 2011;31(4):295-302. doi: 10.1007/s10059-011-0051-5.
9. Szaciłowski K, Macyk W, Drzewiecka-Matuszek A, Brindell M, Stochel G. Bioinorganic photochemistry: frontiers and mechanisms. Chem Rev. 2005;105(6):2647-94. doi: 10.1021/cr030707e.
10. Sunada K, Watanabe T, Hashimoto K. Studies on photokilling of bacteria on TiO2 thin film. J Photochem Photobiol A Chem. 2003;156(1):227-33. doi: 10.1016/s1010-6030(02)00434-3.
11. Yamaguchi K, Sugiyama T, Kato S, Kondo Y, Ageyama N, Kanekiyo M, et al. A novel CD4-conjugated ultraviolet light-activated photocatalyst inactivates HIV-1 and SIV efficiently. J Med Virol. 2008;80(8):1322-31. doi: 10.1002/jmv.21235.
12. Seo JW, Chung H, Kim MY, Lee J, Choi IH, Cheon J. Development of water-soluble single-crystalline TiO2 nanoparticles for photocatalytic cancer-cell treatment. Small. 2007;3(5):850-3. doi: 10.1002/smll.200600488.
13. Belaidi A, Dittrich T, Kieven D, Tornow J, Schwarzburg K, Lux-Steiner M. Influence of the local absorber layer thickness on the performance of ZnO nanorod solar cells. Phys Status Solidi Rapid Res Lett. 2008;2(4):172-4. doi: 10.1002/pssr.200802092.
14. Xu J, Sun Y, Huang J, Chen C, Liu G, Jiang Y, et al. Photokilling cancer cells using highly cell-specific antibody-TiO2 bioconjugates and electroporation. Bioelectrochemistry. 2007;71(2):217-22. doi: 10.1016/j.bioelechem.2007.06.001.
15. Mao C, Xiang Y, Liu X, Cui Z, Yang X, Yeung KWK, et al. Photo-inspired antibacterial activity and wound healing acceleration by hydrogel embedded with Ag/Ag@AgCl/ZnO nanostructures. ACS Nano. 2017;11(9):9010-21. doi: 10.1021/acsnano.7b03513.
16. Qi K, Cheng B, Yu J, Ho W. Review on the improvement of the photocatalytic and antibacterial activities of ZnO. J Alloys Compd. 2017;727:792-820. doi: 10.1016/j.jallcom.2017.08.142.
17. Zhang Z, Zhu Y, Chen X, Zhang H, Wang J. A full-spectrum metal-free porphyrin supramolecular photocatalyst for dual functions of highly efficient hydrogen and oxygen evolution. Adv Mater. 2019;31(7):e1806626. doi: 10.1002/adma.201806626.
18. Yi H, Cheng Z. A literature review on high-performance photocatalysts for sustainable cancer therapy. Crystals. 2021;11(10):1241. doi: 10.3390/cryst11101241.
19. King M, Gee D. Multiscale Modeling of Particle Interactions: Applications in Biology and Nanotechnology. John Wiley & Sons; 2010.
20. Wang J, Fan Y. Lung injury induced by TiO2 nanoparticles depends on their structural features: size, shape, crystal phases, and surface coating. Int J Mol Sci. 2014;15(12):22258-78. doi: 10.3390/ijms151222258.
21. Yamaguchi S, Kobayashi H, Narita T, Kanehira K, Sonezaki S, Kubota Y, et al. Novel photodynamic therapy using water-dispersed TiO2-polyethylene glycol compound: evaluation of antitumor effect on glioma cells and spheroids in vitro. Photochem Photobiol. 2010;86(4):964-71. doi: 10.1111/j.1751-1097.2010.00742.x.
22. Lagopati N, Kitsiou PV, Kontos AI, Venieratos P, Kotsopoulou E, Kontos AG, et al. Photo-induced treatment of breast epithelial cancer cells using nanostructured titanium dioxide solution. J Photochem Photobiol A Chem. 2010;214(2-3):215-23. doi: 10.1016/j.jphotochem.2010.06.031.
23. Lagopati N, Tsilibary EP, Falaras P, Papazafiri P, Pavlatou EA, Kotsopoulou E, et al. Effect of nanostructured TiO_2 crystal phase on photoinduced apoptosis of breast cancer epithelial cells. Int J Nanomedicine. 2014;9:3219-30. doi: 10.2147/ijn.s62972.
24. Lee YS, Yoon S, Yoon HJ, Lee K, Yoon HK, Lee JH, et al. Inhibitor of differentiation 1 (Id1) expression attenuates the degree of TiO2-induced cytotoxicity in H1299 non-small cell lung cancer cells. Toxicol Lett. 2009;189(3):191-9. doi: 10.1016/j.toxlet.2009.05.019.
25. Shukla RK, Sharma V, Pandey AK, Singh S, Sultana S, Dhawan A. ROS-mediated genotoxicity induced by titanium dioxide nanoparticles in human epidermal cells. Toxicol In Vitro. 2011;25(1):231-41. doi: 10.1016/j.tiv.2010.11.008.

26. Hattori K, Nakadate K, Morii A, Noguchi T, Ogasawara Y, Ishii K. Exposure to nano-size titanium dioxide causes oxidative damages in human mesothelial cells: the crystal form rather than size of particle contributes to cytotoxicity. Biochem Biophys Res Commun. 2017;492(2):218-23. doi: 10.1016/j.bbrc.2017.08.054.
27. Zhang AP, Sun YP. Photocatalytic killing effect of TiO2 nanoparticles on Ls-174-t human colon carcinoma cells. World J Gastroenterol. 2004;10(21):3191-3. doi: 10.3748/wjg.v10.i21.3191.
28. Beroukhim R, Getz G, Nghiemphu L, Barretina J, Hsueh T, Linhart D, et al. Assessing the significance of chromosomal aberrations in cancer: methodology and application to glioma. Proc Natl Acad Sci U S A. 2007;104(50):20007-12. doi: 10.1073/pnas.0710052104.
29. D'Cruz AK, Robinson MH, Biel MA. mTHPC-mediated photodynamic therapy in patients with advanced, incurable head and neck cancer: a multicenter study of 128 patients. Head Neck. 2004;26(3):232-40. doi: 10.1002/hed.10372.
30. Popovic EA, Kaye AH, Hill JS. Photodynamic therapy of brain tumors. J Clin Laser Med Surg. 1996;14(5):251-61. doi: 10.1089/clm.1996.14.251.
31. Rozhkova EA, Ulasov I, Lai B, Dimitrijevic NM, Lesniak MS, Rajh T. A high-performance nanobio photocatalyst for targeted brain cancer therapy. Nano Lett. 2009;9(9):3337-42. doi: 10.1021/nl901610f.
32. Ferrari M. Cancer nanotechnology: opportunities and challenges. Nat Rev Cancer. 2005;5(3):161-71. doi: 10.1038/nrc1566.
33. Wang C, Cao S, Tie X, Qiu B, Wu A, Zheng Z. Induction of cytotoxicity by photoexcitation of TiO2 can prolong survival in glioma-bearing mice. Mol Biol Rep. 2011;38(1):523-30. doi: 10.1007/s11033-010-0136-9.
34. Mosmann T. Rapid colorimetric assay for cellular growth and survival: application to proliferation and cytotoxicity assays. J Immunol Methods. 1983;65(1-2):55-63. doi: 10.1016/0022-1759(83)90303-4.
35. Sladowski D, Steer SJ, Clothier RH, Balls M. An improved MTT assay. J Immunol Methods. 1993;157(1-2):203-7. doi: 10.1016/0022-1759(93)90088-o.
36. Cai R, Kubota Y, Shuin T, Sakai H, Hashimoto K, Fujishima A. Induction of cytotoxicity by photoexcited TiO2 particles. Cancer Res. 1992;52(8):2346-8.
37. Stefanou E, Evangelou A, Falaras P. Effects of UV-irradiated titania nanoparticles on cell proliferation, cancer metastasis and promotion. Catal Today. 2010;151(1-2):58-63. doi: 10.1016/j.cattod.2010.02.016.
38. Wang Y, Liu J, Liu L, Sun DD. High-quality reduced graphene oxide-nanocrystalline platinum hybrid materials prepared by simultaneous co-reduction of graphene oxide and chloroplatinic acid. Nanoscale Res Lett. 2011;6(1):241. doi: 10.1186/1556-276x-6-241.
39. Kwon S, Ko H, You DG, Kataoka K, Park JH. Nanomedicines for reactive oxygen species mediated approach: an emerging paradigm for cancer treatment. Acc Chem Res. 2019;52(7):1771-82. doi: 10.1021/acs.accounts.9b00136.
40. Matsunaga T, Tomoda R, Nakajima T, Wake H. Photoelectrochemical sterilization of microbial cells by semiconductor powders. FEMS Microbiol Lett. 1985;29(1-2):211-4. doi: 10.1111/j.1574-6968.1985.tb00864.x.
41. Lopez T, Ortiz E, Alvarez M, Navarrete J, Odriozola JA, Martinez-Ortega F, et al. Study of the stabilization of zinc phthalocyanine in sol-gel TiO2 for photodynamic therapy applications. Nanomedicine. 2010;6(6):777-85. doi: 10.1016/j.nano.2010.04.007.
42. Manthe RL, Foy SP, Krishnamurthy N, Sharma B, Labhasetwar V. Tumor ablation and nanotechnology. Mol Pharm. 2010;7(6):1880-98. doi: 10.1021/mp1001944.